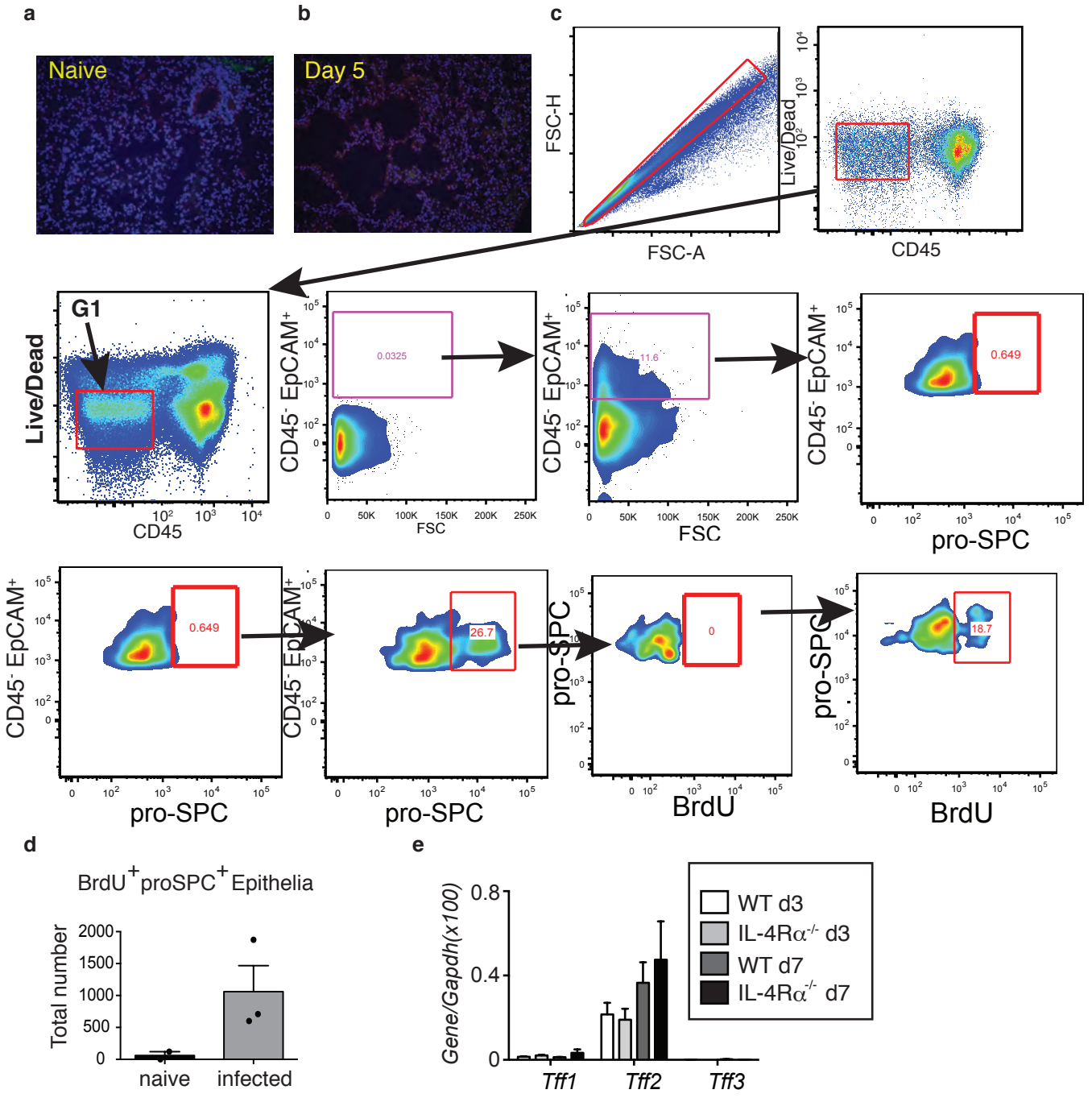

Supplementary Figure 1 Quantification of proliferating epithelial cells during *N.b.* infection and demonstration of IL-4R alpha-independent TFF2 induction.

(**a-b**) Isotype controls for (**a**) naive and (**b**) d5 post-infection of Ym1/Ki-67 staining in **Figure 1c**. Donkey anti-goat (Cy2) and donkey anti-rabbit (Cy3) secondary antibodies were added in the absense of primary antibodies.
(**c**) Flow cytometry gating strategy for the identification of distal lung epithelial cells within single cell suspensions of lung tissue digests: Selection of singlets, fluorescence minus one (FMO) gating for aqua viability dye, dead cell exclusion using aqua viability dye, FMO for CD45$^-$ EpCAM$^+$ epithelia, representative positive staining for EpCAM$^+$ cells, FMO for pro-SPC staining, positive pro-Spc staining, and (**k**) BrdU FMO in the proSPC gate, positive staining for BrDU EpCAM gate.
(**d**) Quantification of total numbers of CD45$^-$ EpCAM$^+$ pro-SPC$^+$ epithelia at d4 following *N.b.* infection. Each symbol represents an individual mouse. (**e**) lung mRNA transcripts for each TFF family member in WT vs IL-4Ra$^{-/-}$mice following *N. b.* infection (N=3-4/group).

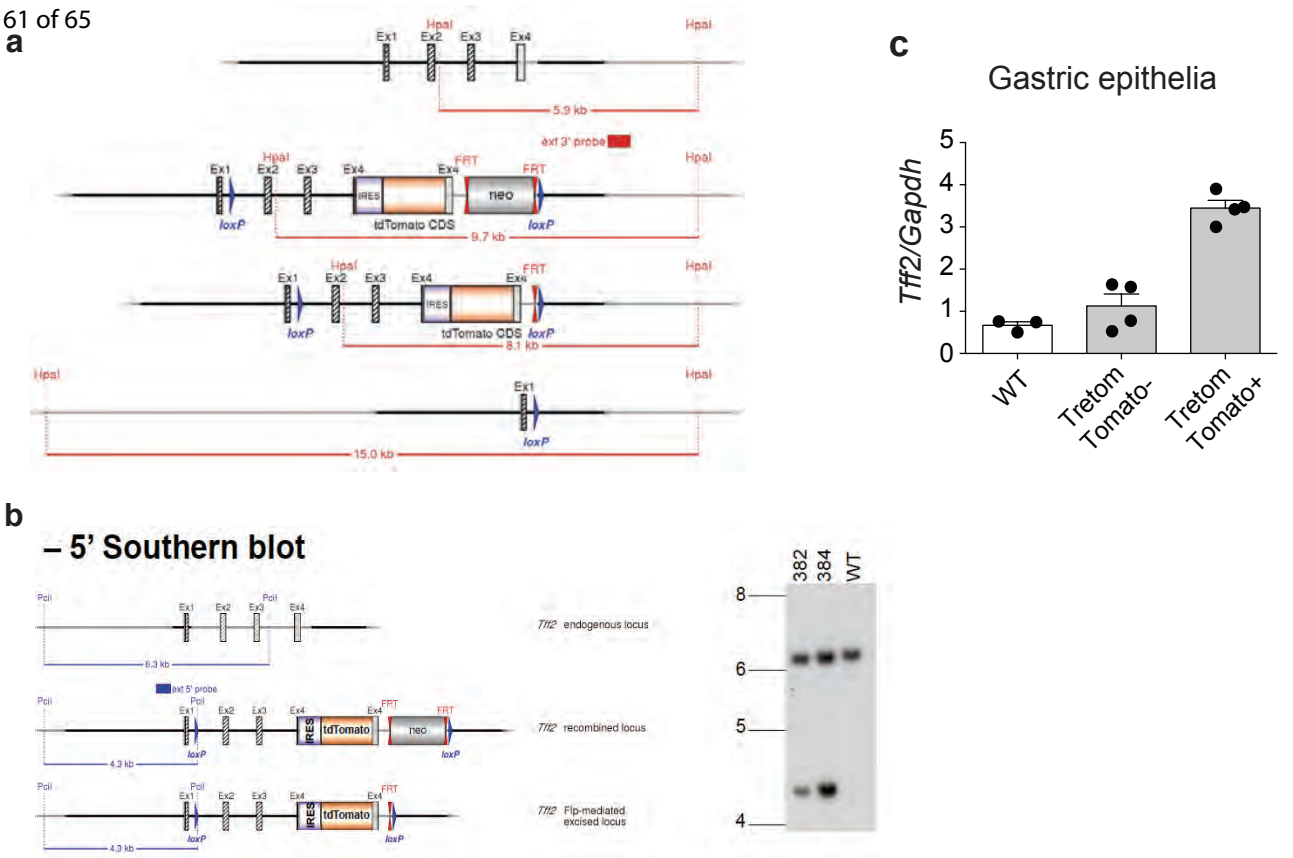

Supplementary Figure 2. TFF2 fluorescent reporter mouse (Tre-Tom) and TFF2 expressing gastric cells

(**a**) Genomic C57BL/6 embryonic stem (ES) cell DNA was used to generate a targeting vector that possessed homology to the single Tff2 isoform that encodes a 129 aa protein (NP_033389). The targeting vector contained long and short homology arms of 6.4 and 1.6kb, respectively, with loxP sites flanking Tff2 exons 2-4 and an IRES td-Tomato reporter downstream of the endogenous STOP codon. Targeted C57BL/6 ES were injected into blastocysts from albino C57BL/6 (C57BL/CJ-Tyrc-2J/J) chimeras identified and bred to deleter strains. Schematic shows the outcome following breeding of Tre-Tom mice with Flp recombinase or cre-deleter strains. (**b**) Southern blot was used to confirm homologous recombination at the 5' end using an internal homology arm to detect Pci generated fragments. (**c**) Expression of *Tff2* in sorted gastric epithelial cells from WT and Tretom reporter mice. Symbols represent individual mouse.

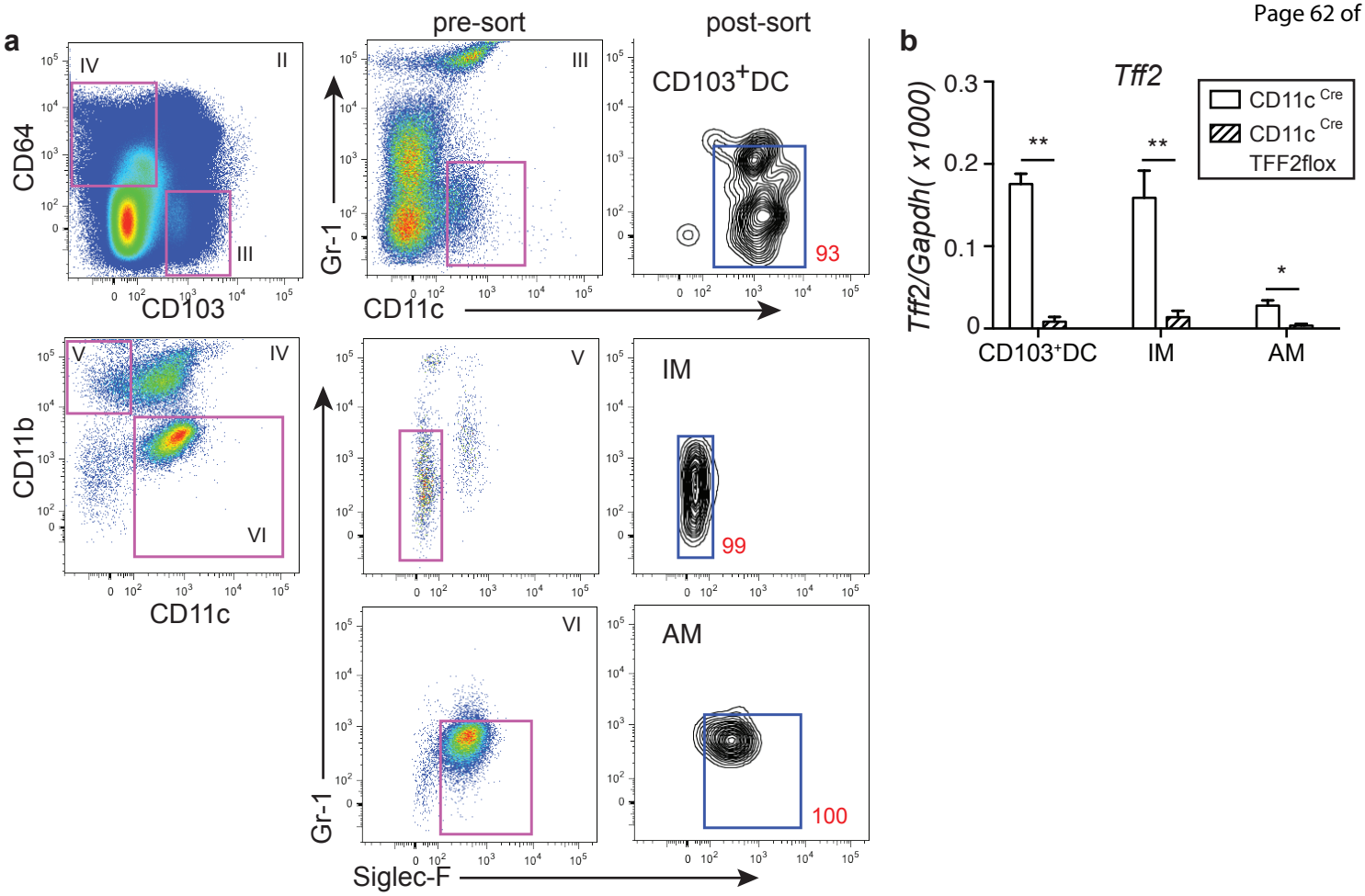

Supplementary Figure 3 Expression of *Tff2* in multiple lung myeloid cells
(**a**) Sorting strategy for lung myeloid cells at d4 following *N.b.* infection. Pre-sort gating and post-sort purity check from a representative mouse are shown. (**b**) *Tff2* expression levels in sorted myeloid subsets in the lung at d4 post-*N.b.* infection. (N=4). *p<0.05 and **, p< 0.01 and ***, p<0.005 as determined by Student's t-test.

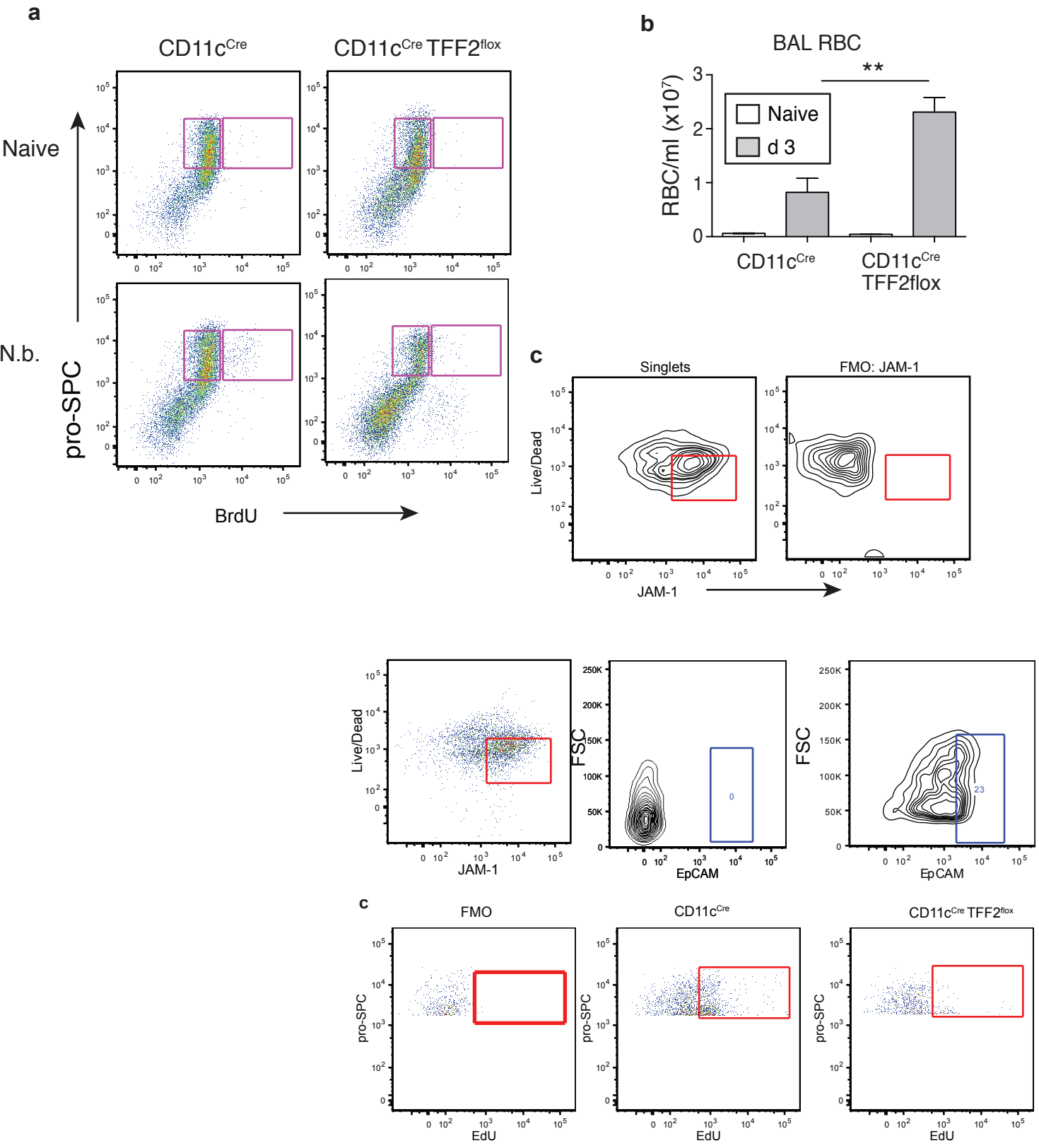

Supplementary Figure 4 TFF2 produced by lung meloid cells is critical in pathogenesis during *N.b.* infection
(a) Representative dot plots showing gating strategy for pro-SPC pos BrdU pos ATII cells pre and post N.b. infection (**b**) Numbers of RBC in BAL fluid at d3 following *N.b.* infection.(**c**) Gating strategy for MERA to identify live JAM-1 postive epithelia recovered from the apical side of the transwell insert. (**c**) EdU FMO for pro-SPC positive cells within the CD45 neg, EpCAM positive pro-SPC pos gate in BrdU experiments at day 9 for Bleomycin experiments.

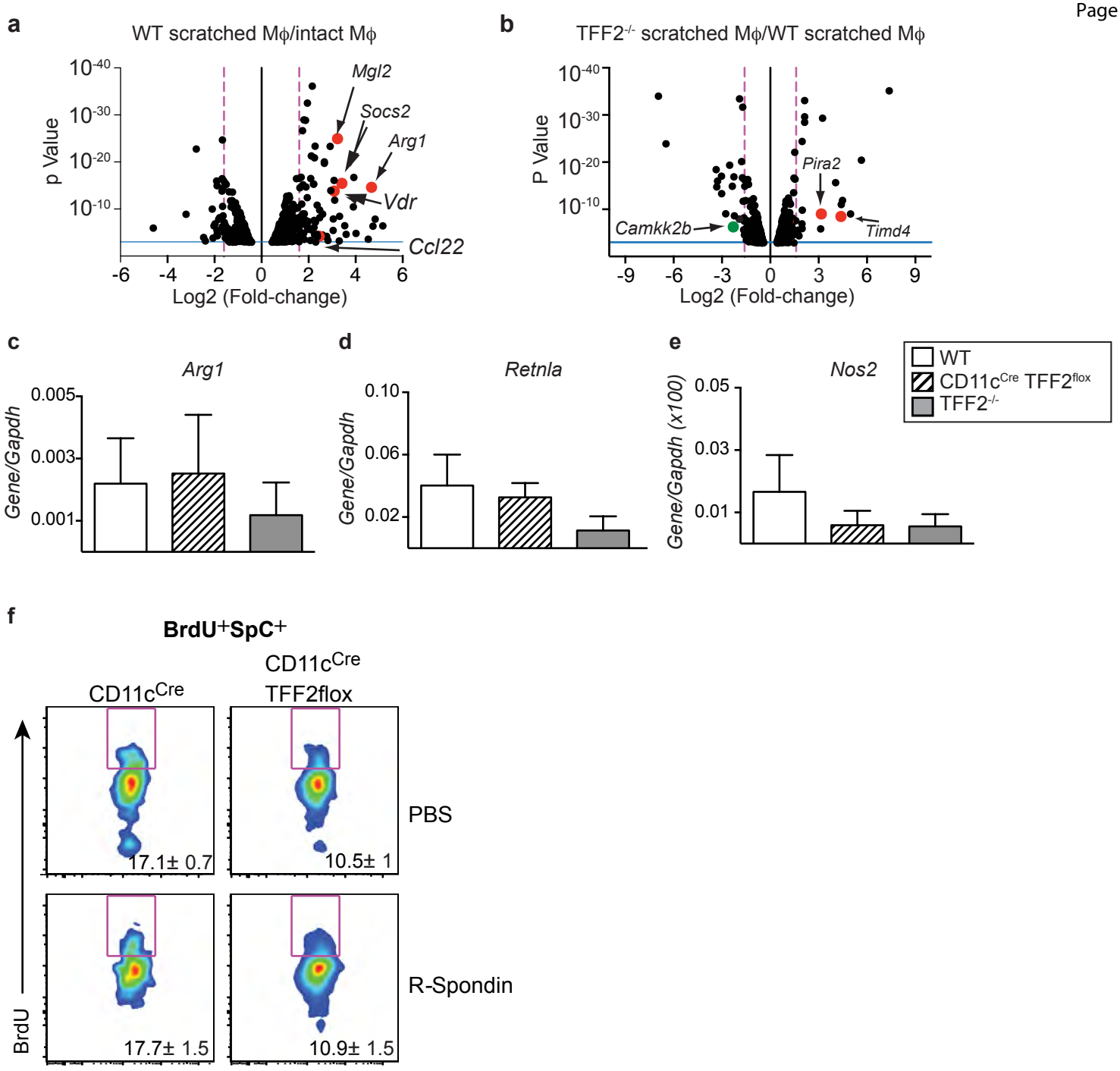

Supplementary Figure 5 Gene expression of BMM or AM upon exposure to injury and the effect of R-spondin on epithelial proliferation after *N.b.* infection

(**a**,**b**) Volcano plots showing results of RNASeq comparing WT BMM recovered from MERA that were exposed to (**a**) intact or scratched MTEC and (**b**) WT or TFF2$^{-/-}$ BMM exposed to damaged MTEC. (**c**-**e**) Sorted AM from WT, CD11c^{Cre}-TFF2flox or TFF2$^{-/-}$ at d4 post-*N.b.* infection were subjected to QRT-PCR to assess (**c**) *Arg1*, (**d**) *Retnla* and (**e**) *Nos2* levels. N=3/group. (**f**) Lungs were collected from CD11c^{Cre} or CD11c^{Cre}-TFF2flox mice, treated with PBS or R-spondin, on d4 post-N.b.infection. Percentages of CD45 neg, EpCAM pos BrdU^{+}SpC^{+} were analyzed by flow cytometry. Numbers indicate mean ± SEM from 5 samples.

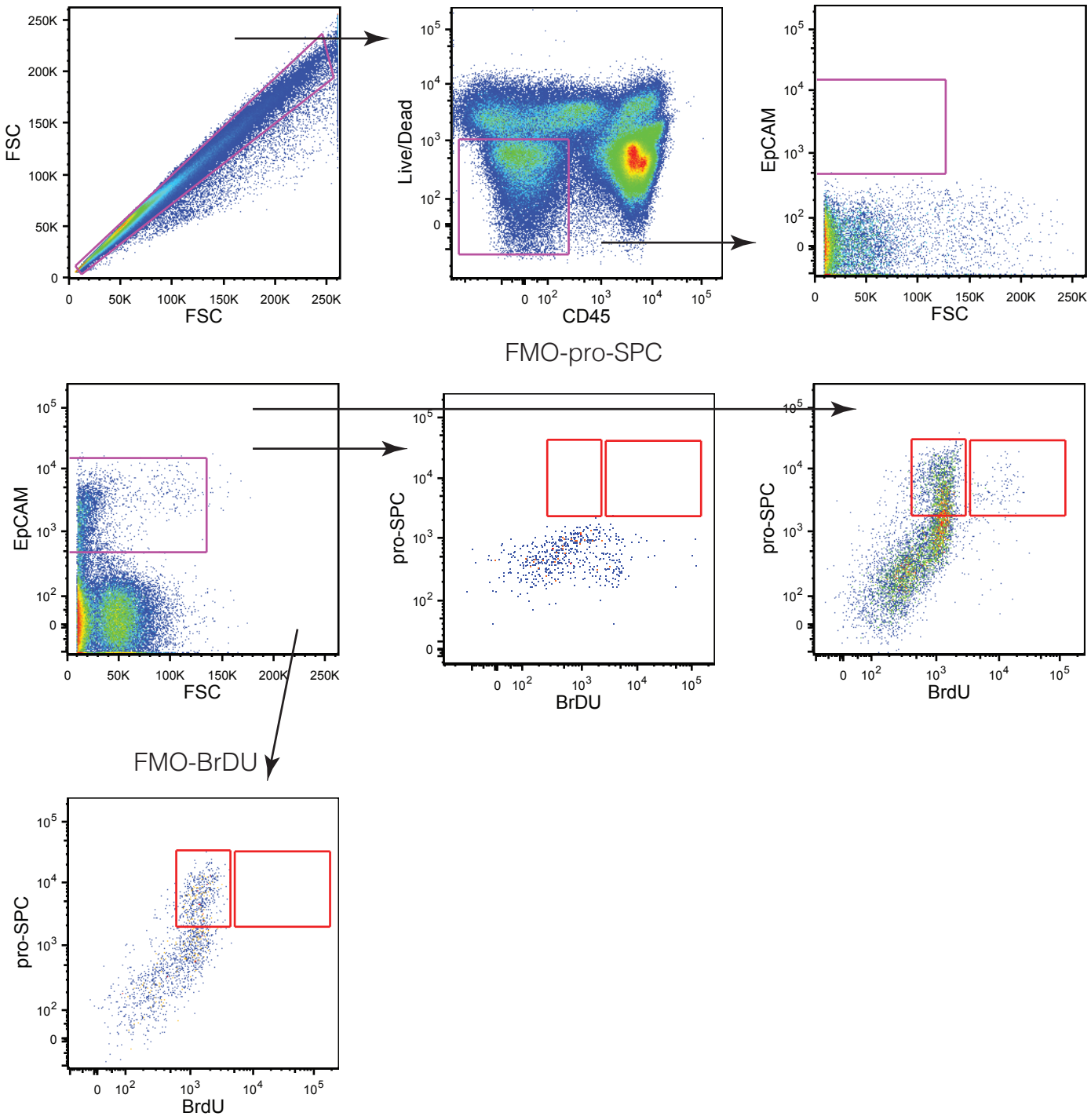

Supplementary Figure 6 Gating ancestry to identify BrdU positive ATII cells

Selection of singlets, dead cell exclusion using aqua viability dye fluorescence minus one (FMO) gating for FMO for $CD45^{-}$ $EpCAM^{+}$ epithelia, representative positive staining for $EpCAM^{+}$ cells,
FMO for pro-SPC staining, positive pro-Spc staining, and (**k**) BrdU FMO in the proSPC gate.